

SUPPLEMENTARY INFORMATION: Band-gap Engineering in methylammonium bismuth bromide for less-toxic perovskite solar cells

Samuel R. Pering^{*1}, Hunaynah Abdulgafar¹⁺, Madeleine Mudd¹, Keith Yendall², Mustafa Togay³ & Mark R.J. Elsegood⁴

¹Department of Materials, Loughborough University, Loughborough, LE11 3TU, UK.

²Loughborough Materials Characterisation Centre, Loughborough, LE11 3TU, UK.

³CREST, Loughborough University, Loughborough, LE11 3TU, UK.

⁴Department of Chemistry, Loughborough University, Loughborough, LE11 3TU, UK.

+ H. Abdulgafar current address: WMG University of Warwick, 6 Lord Bhattacharyya Way, Coventry, CV4 7AL

Samuel R. Pering ORCID ID: 0000-0002-3349-4348

Mark R.J. Elsegood ORCID ID: 0000-0002-8984-4175

EXPERIMENTAL:

Single Crystal Synthesis:

MABr (Ossila, 98%) and BiBr₃ (Merck, 98%) were dissolved in 1 mL of a 7:3 ratio solution of GBL (Alfa Aesar) and DMSO (Alfa Aesar), according to the table below to form a 1 mol solution. A 2:1 ratio of methylammonium halide to bismuth halide was used. The solution was left to evaporate until crystals formed.

Powder Synthesis:

MAI (Ossila, 98%), MABr (Ossila, 98%), BiI₃ (Alfa Aesar, 99.999%) and BiBr₃ (Merck, 98%) were dissolved in 1 mL of a 7:3 ratio solution of GBL (Alfa Aesar) and DMSO (Alfa Aesar), according to the table below to form a 1 mol solution. A 2:1 ratio of methylammonium halide to bismuth halide was used.

Table S1. Masses of material used in precursor solutions

Sample	Mass (mg)			
	MAI	MABr	BiI ₃	BiBr ₃
MA ₃ Bi ₂ I ₉	320.0		590.0	
MA ₃ Bi ₂ (I _{0.8} Br _{0.2}) ₉	256.0	44.8	472.0	89.6
MA ₃ Bi ₂ (I _{0.6} Br _{0.4}) ₉	192.0	89.6	354.0	179.2
MA ₃ Bi ₂ (I _{0.4} Br _{0.6}) ₉	128.0	134.4	236.0	268.8
MA ₃ Bi ₂ (I _{0.2} Br _{0.8}) ₉	64.0	179.2	118.0	358.4
MABiBr ₆		224.0		448.0

Solutions were cast on to glass at 100 °C for 1 hour to form powder samples.

Thin-Film Synthesis:

100 µL of solutions made as above were cast onto static microscope slides or FTO glass (TEC-15, Merck). A spin-coating procedure of 2000 rpm for 20 seconds was used, followed by annealing at 100 °C for 1 hour.

Solar Cell Synthesis:

FTO was etched to the desired pattern using Zn powder (Merck) and 2M HCl (Merck). Substrates were cleaned under sonication at 60 °C using deionised water, acetone, and isopropanol. 35 µL of filtered PEDOT:PSS (Ossila) was spin-coated at 6000 rpm for 40

seconds and heated to 100 °C. 100 μL of perovskite solution was deposited at 2000 rpm for 20 seconds, then annealed at 100 °C for 1 hour. 20 μL of a 20 mgml^{-1} solution of PC₇₁BM (Ossila) was deposited at 3000 rpm for 30 seconds.

80 nm of silver (Alfa Aesar) contacts were deposited by metal evaporation.

Single Crystal XRD:

Diffraction data for single crystal X-ray structure of $[(\text{BiBr}_6^{3-})(\text{H}_3\text{CNH}_3^+)] \cdot 2(\text{CH}_3)_2\text{SO}$ (**1**) was collected on a Rigaku FRE+ diffractometer equipped with Arc)Sec VHF Varimax confocal mirrors and HyPix 6000HE detector.¹ The structure was solved by a dual-space charge-flipping algorithm and refined by full-matrix least-squares.^{2,3} Crystal details and information about the data collection and refinement are provided in Table S2, below. A quarter of the formula is unique. The DMSO was two-fold disordered over a symmetry element, so was refined at half-weight. The methylammonium cations were substantially disordered with Me and NH₃ groups interchanged while these cations also resided on symmetry elements. Thus, not all H atoms could be located/modelled, but are included in the formula.

CCDC 2265208 contains the supplementary crystallographic data for this paper. These data can be obtained free of charge from The Cambridge Crystallographic Data Centre via www.ccdc.cam.ac.uk/structures.

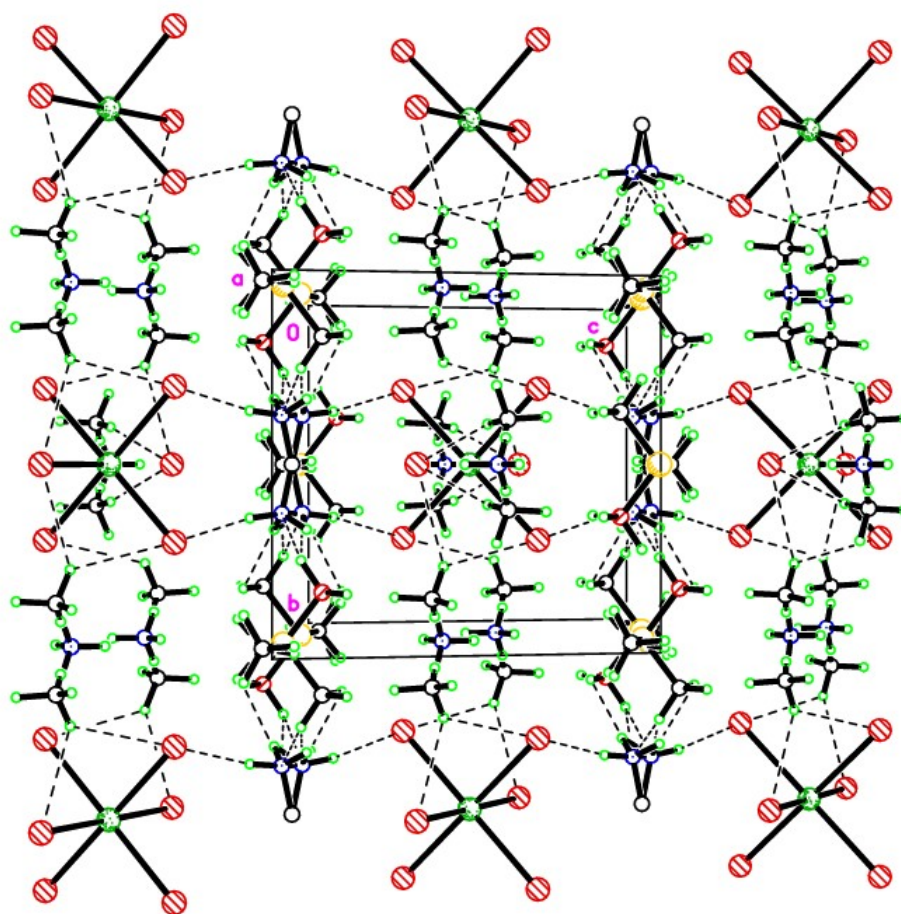


Figure S1. Packing plot of **1** viewed parallel to the *a* axis.

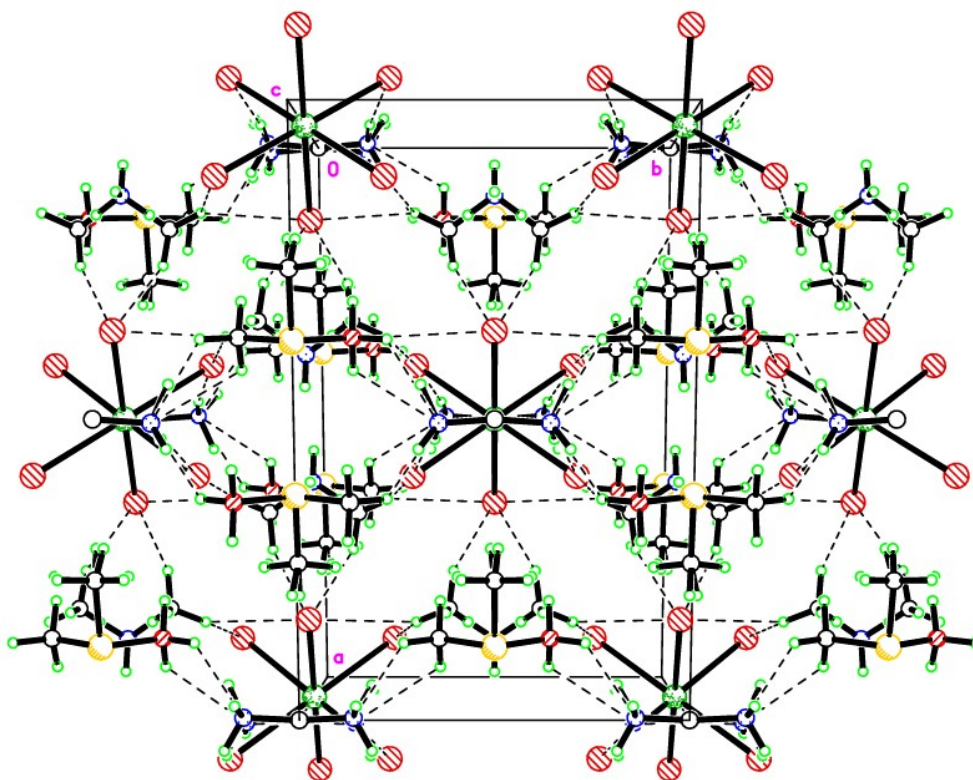


Figure S2. Packing plot of **1** viewed parallel to the *c* axis

Table S2. Crystal data for **1**.

Crystal data

(BiBr ₆ ³⁻)·3(CH ₆ N ⁺)·2(C ₂ H ₆ OS)	<i>F</i> (000) = 868
<i>M_r</i> = 940.90	<i>D_x</i> = 2.495 Mg m ⁻³
Monoclinic, <i>C2/m</i>	Mo <i>K</i> α radiation, λ = 0.71073 Å
<i>a</i> = 14.5874 (4) Å	Cell parameters from 8059 reflections
<i>b</i> = 9.2026 (2) Å	θ = 2.6–31.6°
<i>c</i> = 9.5884 (3) Å	μ = 16.78 mm ⁻¹
β = 103.333 (3)°	<i>T</i> = 100 K
<i>V</i> = 1252.47 (6) Å ³	Block, clear colourless
<i>Z</i> = 2	0.21 × 0.14 × 0.09 mm ³

Data collection

Rigaku FRE+ equipped with Arc)Sec VHF Varimax confocal mirrors and an UG2 goniometer and HyPix 6000HE detector diffractometer	2171 independent reflections
Radiation source: Rotating Anode	2106 reflections with <i>I</i> > 2σ(<i>I</i>)
Detector resolution: 10 pixels mm ⁻¹	<i>R</i> _{int} = 0.038

profile data from ω -scans	$\theta_{\max} = 31.7^\circ$, $\theta_{\min} = 2.2^\circ$
Absorption correction: analytical. <i>CrysAlis PRO</i> 1.171.41.113a (Rigaku Oxford Diffraction, 2021). Analytical numeric absorption correction using a multifaceted crystal model based on expressions derived by R.C. Clark & J.S. Reid. (Clark, R. C. & Reid, J. S. (1995). <i>Acta Cryst. A</i> 51, 887-897). Empirical absorption correction using spherical harmonics, implemented in SCALE3 ABSPACK scaling algorithm.	$h = -21 \rightarrow 21$
$T_{\min} = 0.072$, $T_{\max} = 0.210$	$k = -13 \rightarrow 13$
54706 measured reflections	$l = -13 \rightarrow 13$

Refinement

Refinement on F^2	Secondary atom site location: difference Fourier map
Least-squares matrix: full	Hydrogen site location: mixed
$R[F^2 > 2\sigma(F^2)] = 0.020$	H atoms treated by a mixture of independent and constrained refinement
$wR(F^2) = 0.042$	$w = 1/[\sigma^2(F_o^2) + (0.0119P)^2 + 9.1935P]$ where $P = (F_o^2 + 2F_c^2)/3$
$S = 1.08$	$(\Delta/\sigma)_{\max} = 0.001$
2171 reflections	$\Delta\rho_{\max} = 1.53 \text{ e } \text{\AA}^{-3}$
79 parameters	$\Delta\rho_{\min} = -1.54 \text{ e } \text{\AA}^{-3}$
6 restraints	Extinction correction: <i>SHELXL2018/3</i> (Sheldrick 2018), $F_c^* = kF_c [1 + 0.001x F_c^2 \lambda^3 / \sin(2\theta)]^{-1/4}$
Primary atom site location: iterative	Extinction coefficient: 0.00041 (6)

Thin-film/Powder: A Bruker D2 System was used for structural measurements, using a Cu source. Scans were taken from 5° to 50° .

UV/Vis:

UV/Vis measurements were carried out on a Cary5000 UV/Vis spectrophotometer, scanning from 900 nm to 300 nm in reflectance mode.

Microscopy:

AFM measurements were performed using a Bruker Bioscope Resolve in Dynamic mode. SEM Measurements were made on a JEOL 7100F.

PV Characterisation: The J-V characteristics were measured using an in-house solar simulator setup in the dark and under illumination with AM1.5G spectral match, calibrated using a reference Si photodiode. Measurements were taken at 1 Sun illumination. Simulator uses a xenon arc lamp, and all the measurements were performed at room temperature.

RESULTS:

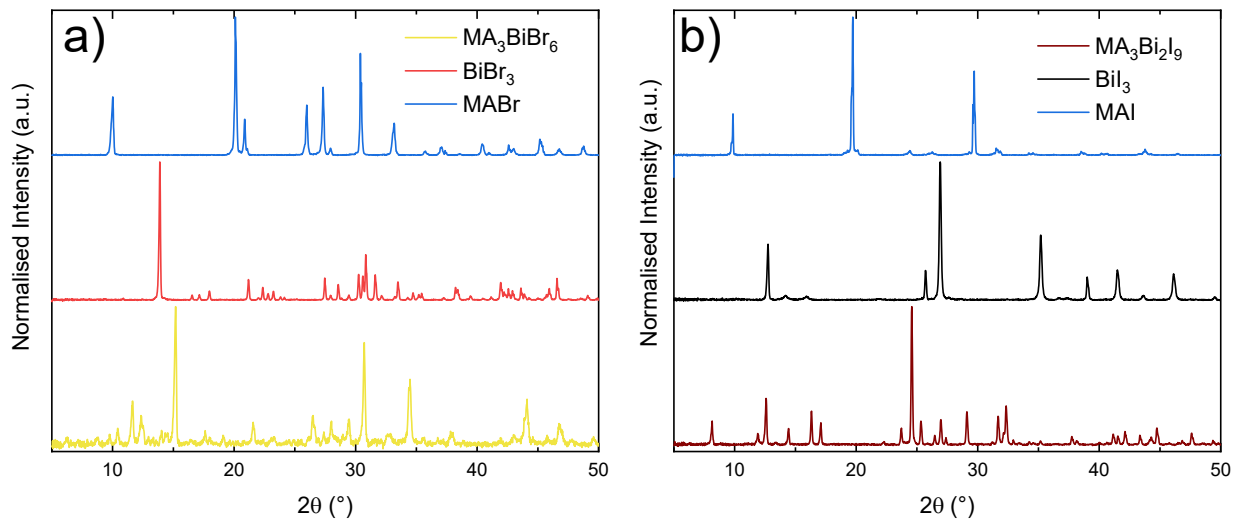


Figure S3. X-ray diffractograms of powder samples against starting materials for a) MA_3BiBr_6 , and b) $MA_3Bi_2I_9$.

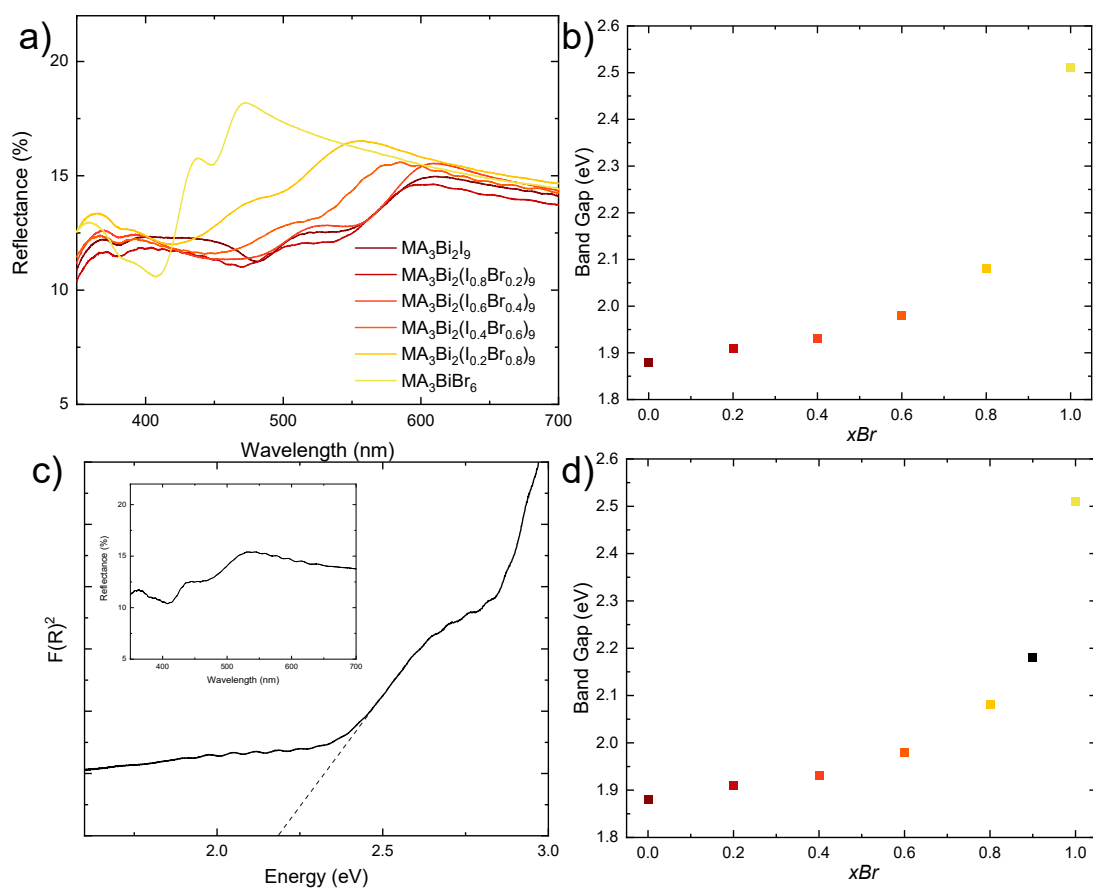


Figure S4. a) Diffuse Reflectance Spectroscopic Analysis of methylammonium bismuth halide Materials, b) Trend of band gap with increasing mole fraction bromide c) Kubelka-Munk function for $\text{MA}_3\text{Bi}_2(\text{I}_{0.1}\text{Br}_{0.9})_9$ with inset reflectance, and d) Trend of band gap with increasing mole fraction bromide with $\text{MA}_3\text{Bi}_2(\text{I}_{0.1}\text{Br}_{0.9})_9$ data included.

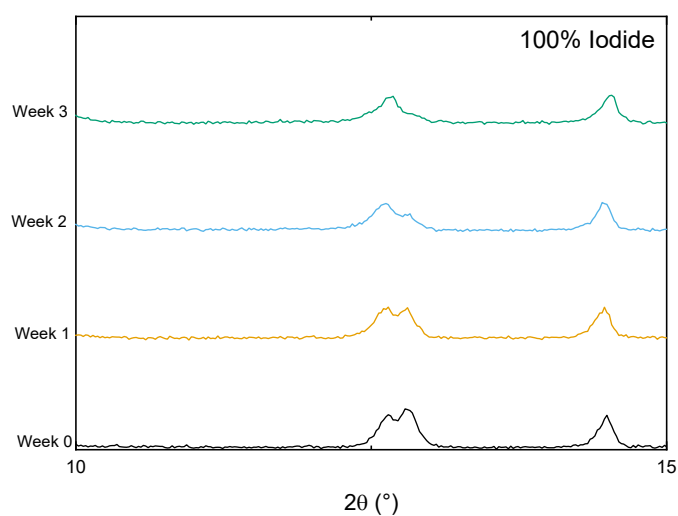


Figure S5. Zoomed in image for $\text{MA}_3\text{Bi}_2\text{I}_9$ of the first three weeks showing the disappearance of the split peak

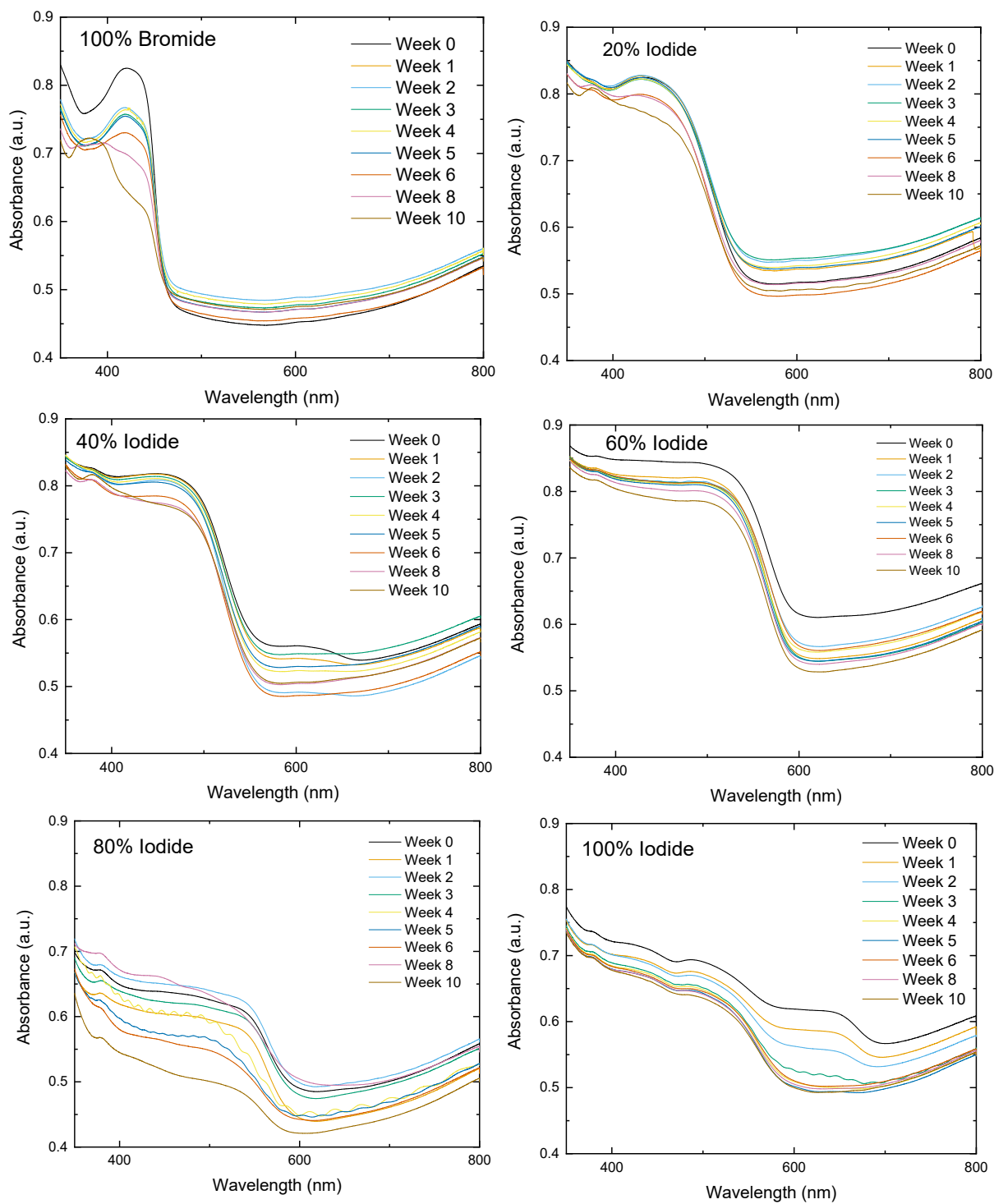


Figure S6. 10 week stability study of thin-films through UV/Vis spectroscopy. Graph headings correspond to the proportion of iodide or bromide in the sample.

MICROSCOPY:

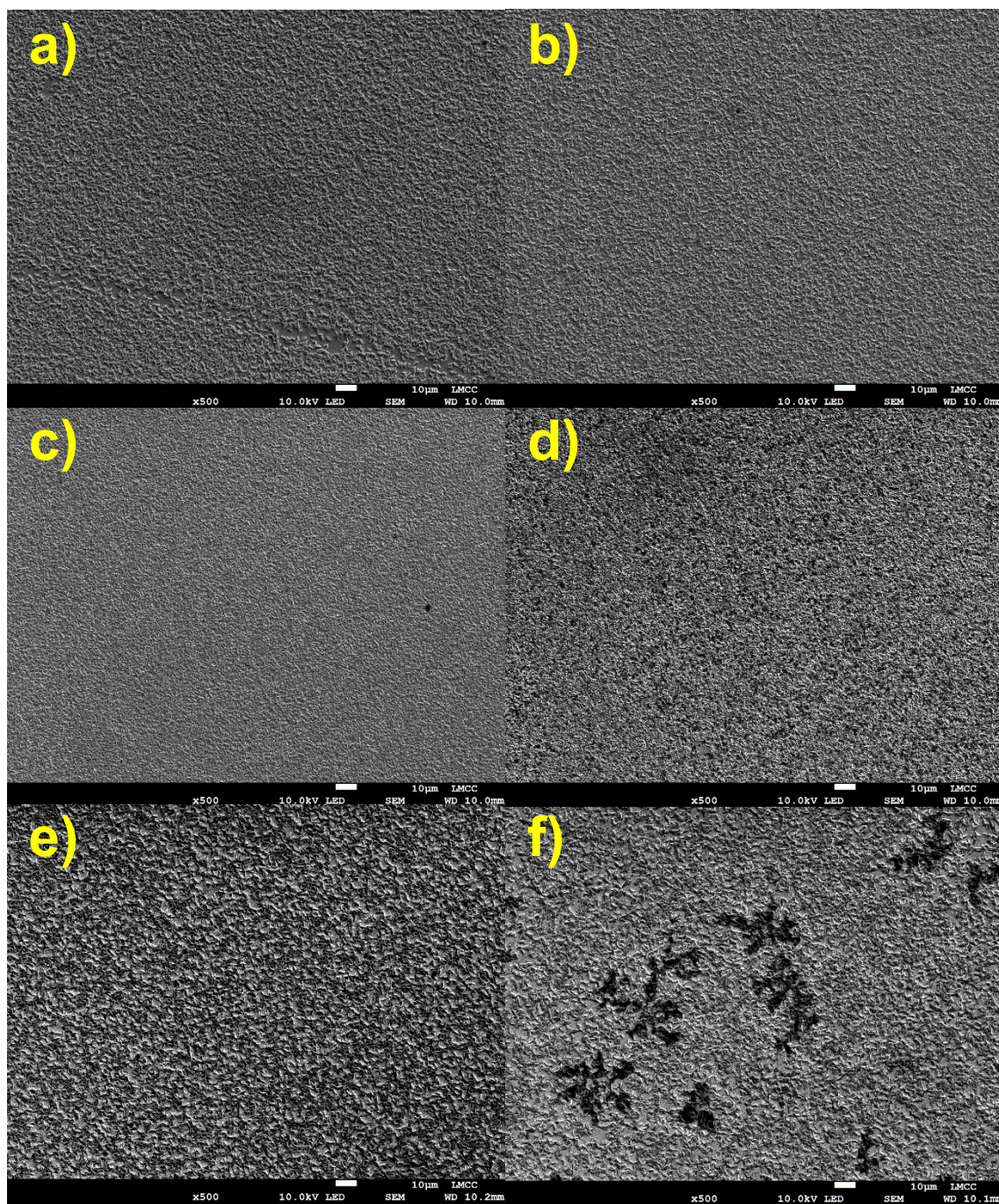


Figure S7. SEM Images at 500x magnification of methylammonium bismuth halide films, 10 μm x 10 μm : a) $\text{MA}_3\text{Bi}_2\text{I}_9$, b) $\text{MA}_3\text{Bi}_2(\text{I}_{0.8}\text{Br}_{0.2})_9$, c) $\text{MA}_3\text{Bi}_2(\text{I}_{0.6}\text{Br}_{0.4})_9$, d) $\text{MA}_3\text{Bi}_2(\text{I}_{0.4}\text{Br}_{0.6})_9$, e) $\text{MA}_3\text{Bi}_2(\text{I}_{0.2}\text{Br}_{0.8})_9$, and f) MA_3BiBr_6 .

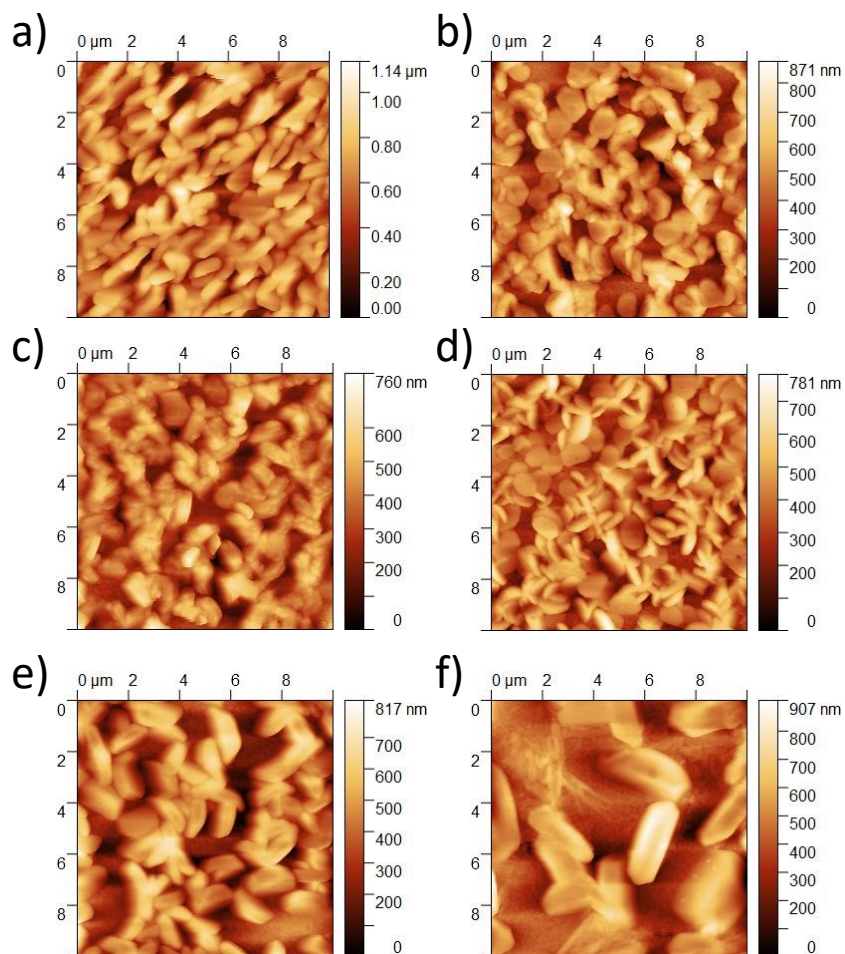


Figure S8. AFM Images of methylammonium bismuth halide films, $10\ \mu\text{m} \times 10\ \mu\text{m}$: a) $\text{MA}_3\text{Bi}_2\text{I}_9$, b) $\text{MA}_3\text{Bi}_2(\text{I}_{0.8}\text{Br}_{0.2})_9$, c) $\text{MA}_3\text{Bi}_2(\text{I}_{0.6}\text{Br}_{0.4})_9$, d) $\text{MA}_3\text{Bi}_2(\text{I}_{0.4}\text{Br}_{0.6})_9$, e) $\text{MA}_3\text{Bi}_2(\text{I}_{0.2}\text{Br}_{0.8})_9$, and f) MA_3BiBr_6 .

Table S3. Average Grain Size of a sample of 10 random grains taken from each AFM image.

Sample	Average Grain Size (μm)
$\text{MA}_3\text{Bi}_2\text{I}_9$	1.0 ± 0.17
$\text{MA}_3\text{Bi}_2(\text{I}_{0.8}\text{Br}_{0.2})_9$	0.99 ± 0.18
$\text{MA}_3\text{Bi}_2(\text{I}_{0.6}\text{Br}_{0.4})_9$	0.95 ± 0.15
$\text{MA}_3\text{Bi}_2(\text{I}_{0.4}\text{Br}_{0.6})_9$	1.1 ± 0.13
$\text{MA}_3\text{Bi}_2(\text{I}_{0.2}\text{Br}_{0.8})_9$	1.4 ± 0.20
MA_3BiBr_6	2.8 ± 0.38

a)

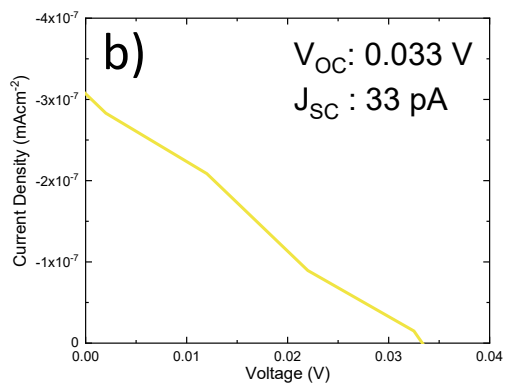
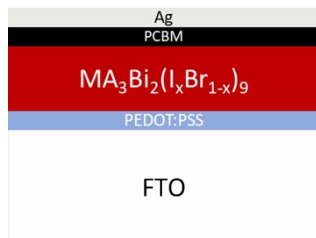


Figure S9. a) Schematic of solar cell, and b) JV curve for MA_3BiBr_6 with inset open-circuit voltage and short-circuit current density.

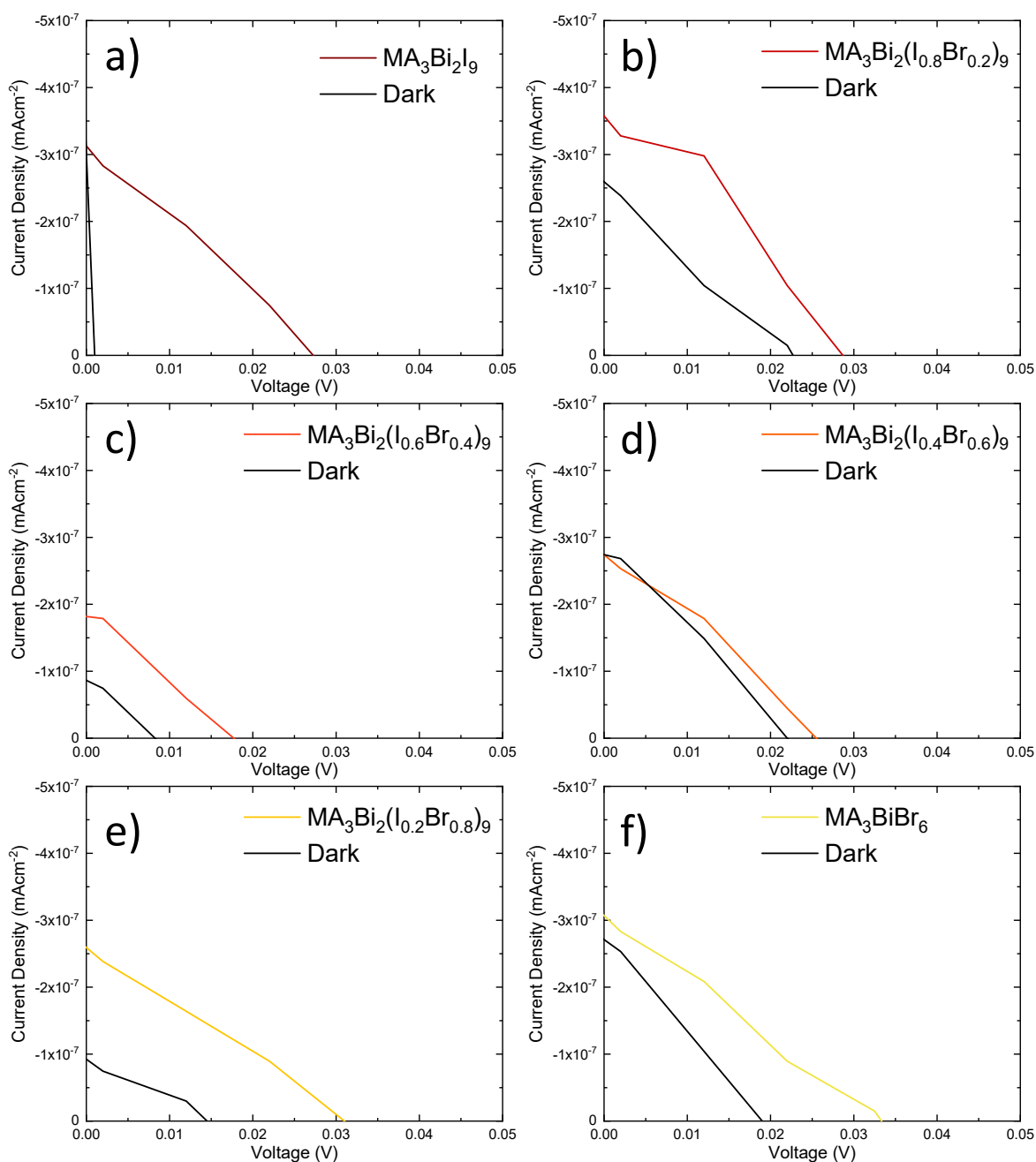


Figure S10. JV curves of methylammonium bismuth halide films: a) $\text{MA}_3\text{Bi}_2\text{I}_9$, b) $\text{MA}_3\text{Bi}_2(\text{I}_{0.8}\text{Br}_{0.2})_9$, c) $\text{MA}_3\text{Bi}_2(\text{I}_{0.6}\text{Br}_{0.4})_9$, d) $\text{MA}_3\text{Bi}_2(\text{I}_{0.4}\text{Br}_{0.6})_9$, e) $\text{MA}_3\text{Bi}_2(\text{I}_{0.2}\text{Br}_{0.8})_9$, and f) MA_3BiBr_6 . All efficiencies are below $5 \times 10^{-5} \%$ and therefore photovoltaic parameters have not been included.

References:

1. CrysAlis PRO software, v1.171.4113a, Rigaku Oxford Diffraction, 2021.
2. SHELXT G.M. Sheldrick, *Acta Cryst.* (2015), **A71**, 3-8.
3. SHELXL (since 2008) G.M. Sheldrick, *Acta Cryst.* (2015), **C71**, 3-8.